

# Segmentation Method of Time-Lapse Microscopy Images with the Focus on Biocompatibility Assessment

Jindřich Soukup<sup>1,2,3,\*</sup>, Petr Císař<sup>1</sup>, Filip Šroubek<sup>3</sup>

1 Institute of Complex Systems FFPW, CENAKVA, University of South Bohemia

Zámek 136, CZ-373 33, Nové Hrady, Czech Republic

2 Faculty of Mathematics and Physics, Charles University in Prague

Ke Karlovu 3, CZ-121 16, Prague 2, Czech Republic

3 Department of Image Processing, Institute of Information Theory and Automation of the ASCR

Pod vodárenskou věží 4, CZ-182 08, Prague 8, Czech Republic

\* E-mail: jindra@matfyz.cz Phone number: +420 777 906 067

## Abstract

Biocompatibility testing of new materials is often performed in vitro by measuring the growth rate of mammalian cancer cells in time-lapse images acquired by phase contrast microscopes. The growth rate is measured by tracking cell coverage, which requires an accurate automatic segmentation method. However, cancer cells have irregular shapes that change over time, the mottled background pattern is partially visible through the cells and the images contain artifacts such as halos.

We developed a novel algorithm for cell segmentation that copes with the mentioned challenges. It is based on temporal differences of consecutive images and a combination of thresholding, blurring and morphological operations. We tested the algorithm on images of four cell types acquired by two different microscopes, evaluated the precision of segmentation against manual segmentation performed by a human operator and finally provided comparison with other freely available methods. We propose a new, fully automated method for measuring the cell growth rate based on fitting a coverage curve with the Verhulst population model.

The algorithm is fast and shows accuracy comparable to manual segmentation. Most notably it can correctly separate live from dead cells.

## Author Summary

### 1 Introduction

Computer processing of microscopy images is currently a popular topic in image-based system biology. Time consuming and subjective manual processing by human experts is

being progressively replaced by automated techniques, that not only save time but also achieve superior results.

A common task motivated by the development of body implants is to determine biocompatibility or cytotoxicity of various materials. The human body is extremely sensitive to foreign materials. Implants made of unsuitable materials may cause severe immune reactions, yet clinical material testing is costly and time consuming. Therefore, researchers are attempting to develop methods of *in vitro* material testing. One of the possible methods of cytotoxicity analysis is based on the cell proliferation monitored by the time-lapse microscopy. A visual inspection of the cell growth or cell dilatation is used as a measure of the cytotoxicity level. [Chen and Chen, 1981, Červinka and Půža, 1990] Testing is performed with cancer cells which are easy to grow *in vitro*. [Masters, 2002]

To achieve the highest fidelity, the least invasive capture method ought to be selected. A common choice is a microscope based on the phase contrast principle (PC microscope). Unlike fluorescence microscopes, phase contrast does not require any labeling of cells; moreover, it uses a reasonable amount of light and provides high-contrast images of the cell interior. Unfortunately, the resulting images contain artifacts such as bright areas around the cell borders – halos.

Determining the growth rate is a well-defined task that can be automated using a computer, which thus significantly saves time compared to manual processing. In the first step, it is necessary to distinguish the cells from the background and then compute the growth rate from the evolution of the area size occupied by the cells. Unlike humans, computers are not automatically capable of distinguishing cells from the background. Segmentation by itself is a complex task and in our case it is even more complicated due to several factors, such as the presence of impurities in the solution, poorly focused specimen, shallow depth of focus of microscope images, presence of halos or texture-like background of images (see image examples in Fig. 1). Also distinguishing the dead live from dead (without labeling with trypan blue which would affect the cells' behaviour during the experiment) is a difficult task.

We cannot use classical segmentation methods like thresholding or the watershed method, however, the literature mentions several approaches:

Active contours and levelset methods are relatively slow [Seroussi et al., 2012, Ambühl et al., 2012, Li et al., 2009] and must be initialized manually or by some other method [Li et al., 2006, Peng et al., 2009, Ersoy et al., 2008]. Problems with cell clustering, halos around cells and the change of area topology covered by cells must be treated. [Zimmer et al., 2002] The quality of segmentation depends on the initialization and in the case of manual initialization the results are poorly reproducible.

Methods based on machine learning [Yin et al., 2010, Pan et al., 2010, 2009] depend on the cell and microscope type. These methods can achieve satisfactory results, yet high quality and comprehensive learning data set ought to be provided.

Recently, a novel method [Yin and Kanade, 2011, Kanade et al., 2011, Yin et al., 2012] has been developed based on removing artifacts from images. The authors assume

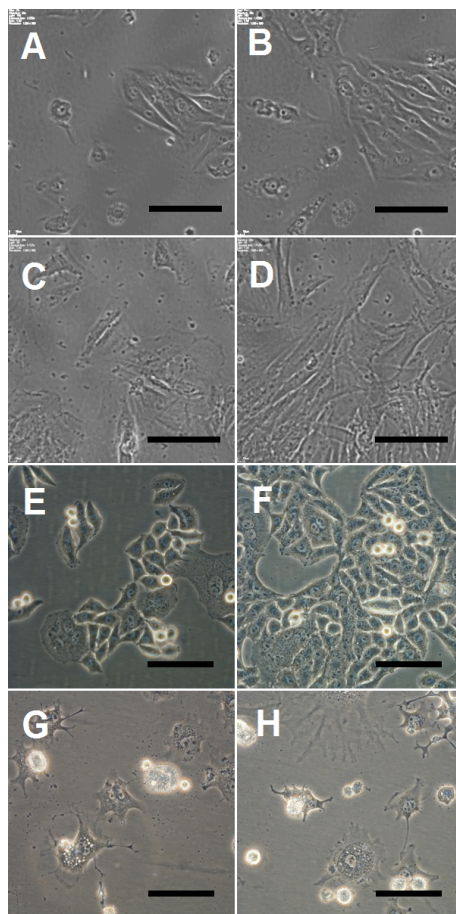


**Figure 1.** Examples of tested samples: A, B - MG63 cells, Nikon Biostation microscope (A - poorly focused); C, D - G10 cells, Nikon Biostation microscope (impurities in solution - black dots outside the cells); E, F - L929 cells (irregular shapes of cells, dead cells), Olympus microscope (texture-like background, strong halos); G, H - HeLa cells, Olympus microscope.

that artifacts present in images from a PC microscope could be described by degradation (convolution) of the original image with the known impulse response. Using a deconvolution algorithm they can obtain a modified image which no longer contains halos around cells. Segmentation is then performed by simple thresholding. The disadvantage of this method is the instability of deconvolution. To obtain acceptable results regularization and advanced optimization methods must be applied.

The last main group of methods (e.g. [Bradhurst et al., 2008, Huth et al., 2010, Juneau et al., 2013]) is based on image filtering and consecutive thresholding. However, these methods often fail to provide accurate segmentation if images have either very small or very high coverage. We propose a novel method that belongs to this group, solves problems with the low and high coverage and, moreover, can distinguish dead live from dead cells. Compared to the active contours, our method is fast, it is also versatile and highly accurate.

The rest of the paper is organized as follows. The next section describes in detail our segmentation algorithm which was previously outlined in [Soukup et al., 2013]. The following sections provide evaluation of the accuracy of our algorithm (sections 3.2 and 3.1) and offer application in biotoxicity assessment (section 3.3 and 3.4). Finally, a brief summary of the paper is presented in the last section.

## 2 Methods

Prior to the method description, we first discuss our assumptions. We process a series of time-lapse images and assume that (1) all images capture the same area (all images are registered – geometrically aligned), (2) luminosity changes in images do not occur (such as automatic white balance and contrast correction), (3) the background (area without cells) is still in time and changes only due to noise, (4) movement of cells as well as movement of cell’s interior can be observed and (5) only minor cell coverage differences between consecutive images are present (our method works well only when the frame rate of time-lapse capturing is sufficient – frequency of capturing depends on the type of cells and on microscope magnification; capturing one image per hour usually suffices).

These five assumptions are necessary for correct functionality of our method. Assumptions (1) and (3) are crucial and their violation will render the method useless. The remaining three assumptions are not so critical yet they influence the method’s precision. However, all the assumptions are typically fulfilled or can be guaranteed when using a proper experimental setting. The method is well suitable for routine use in laboratory practice.

Our method consists of several steps that can be grouped into three phases – preprocessing, thresholding and correction. In the preprocessing phase we change image modality to improve the contrast between areas with/without cells. The thresholding phase consists of dividing the image into areas with/without cells (segmentation) and the

correction phase improves segmentation using several heuristics (see Fig. 2).

## 2.1 Preprocessing

Images from the phase contrast microscope have poor contrast between cell and background regions and thus simple segmentation methods cannot be applied. However, if the absolute value of differences of two consecutive images is taken into account, the contrast between the cells and the background is clearly visible. Here we make use of assumptions (3) and (4). When the background is still, the differences between two consecutive images are small (and depend only on the level of noise). On the other hand, when movement inside the cells is observed, the brightness is changing and higher differences between consecutive images in those areas are more apparent.

The result of this step is a texture-like image that consists of regions with very low intensity values (background) and regions with both high and low intensity values (cells). The contrast in these two regions depends on the time interval between capturing these two images. When the frame rate is very high, the position of cells changes only very little. In this case we cannot compare two consecutive images but images more distant in time ought to be utilized. A low frame rate poses a more serious problem. When the time interval between two images is too long, cells might migrate to a completely new position. After the difference step, we will detect response at both the initial and final position of the cells. This kind of problem can be partially solved in the correction phase (see Sec. 2.3), however, it yields the entire algorithm less precise. One can observe that the selected time step utilized for the calculation of the differences influences the correct functionality of the algorithm.

The second step consists of blurring the difference image. The background regions remain unchanged and the cell regions become more homogenous (see Fig. 2). We apply Gaussian blurring with a very small kernel (standard deviation 1, kernel mask  $3 \times 3$ ).

The last step in the preprocessing phase is thresholding. We assume that coverage in the current image will be similar to the previous image and this information is used for setting the threshold value. When the coverage in previous images was  $C$  %, in this step we set the threshold value as the  $C$ -th quantile of the image histogram. Thus  $C$  % of pixels with the highest values become white and the rest  $(100 - C)$  % black. In this way we increase the contrast between the regions that we want to separate (see Fig. 2).

When the assumption (5) concerning moderately changing coverage is not fulfilled, this step of the algorithm can lead to an underestimated coverage increase/shrinkage. To our knowledge this assumption holds whenever the frame rate is sufficiently high and the preprocessing phase works because movement inside the cells and migration of the cells is faster than the cells growth.

In summary, three operations are being applied (difference of consecutive images, blurring and thresholding) to increase the contrast between the cells and the background

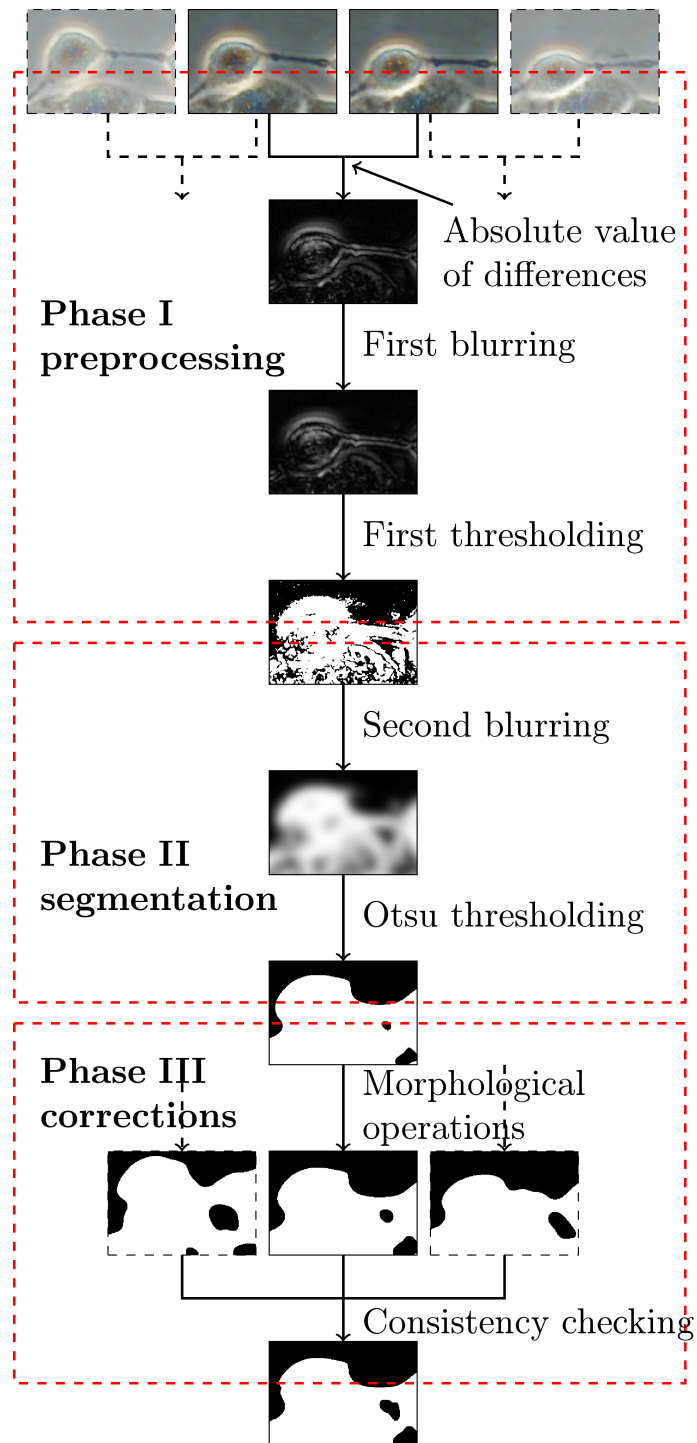


Figure 2. Pipeline of our algorithm.

compared to the original image. This allows a successful application of a very simple segmentation method in the next phase of the algorithm.

## 2.2 Segmentation

The segmentation phase consists of two steps – blurring and thresholding. Blurring serves to fill small holes in otherwise uniform regions. The holes may correspond to debris moving in the background or, for example, to a cell nucleus which remained stationary between the last two frames. In this case blurring plays a different role than in the preprocessing phase and, therefore, the blurring parameters differ. This time we use gaussian blur with a larger standard deviation which depends on microscope magnification and should be set between quarter to half of the smallest cell’s diameter.

After blurring, the modified Otsu thresholding is applied. The original Otsu thresholding automatically chooses a threshold value using only the image histogram. The threshold value is set to maximize separability between two resulting (background/foreground) classes [Otsu, 1975]. When two areas are approximately of the same size, Otsu thresholding functions properly. A problem occurs when one region is significantly smaller than the other. In these cases Otsu thresholding fails to locate the optimal threshold near the margins of the histogram and selects a point in the center of the histogram instead.

We modified Otsu thresholding to prevent this false behavior. When coverage  $C$  in the previous image is too high or too low we apply Otsu thresholding only on a part of the histogram. Then the optimal value will be closer to the center of the cropped histogram and the algorithm selects the optimal thresholding value. (If coverage in the previous frame is between 0.25 and 0.75, we apply Otsu thresholding to the whole histogram. Above and below this range we process only  $100 \cdot 16 \cdot (1 - C)^2$  % and  $100 \cdot 16 \cdot C^2$  % of the histogram respectively.) This modification significantly improves the segmentation precision in images with very small or very high coverage. After this step we obtain a very good approximation of the ground truth segmentation.

## 2.3 Correction Phase

This phase handles certain irregularities in data and thus improves the segmentation quality. Possible sources of irregularities are debris in liquid, ghost images of out-of-focus objects or discrepancies caused by rapid cell movement (for example shrinking/spreading before/after cell mitosis). First we apply a morphological operation erosion to move the pixels affected by the halo effect from the cells area to the background. We also remove objects smaller than the minimum cells size by labeling the cells area and counting the number of pixels in individual segments. Then we compare labeling of pixels in the neighboring images in time. Pixels labeled as cells only in the current image belong very probably to certain irregularities such as ghost images of out-of-focus objects. In this case we reclassify such pixels as background despite their original classification.

## 2.4 Further Notes on the Algorithm

Our algorithm uses the coverage  $C$  of the previous frame in each step. This information is not available when processing the first frame and, therefore, we restart the segmentation process several times. In the first run an arbitrary  $C$  is chosen (human operator input or a 0.5 value) and in the following runs the coverage of the last frame before the restart is used. The initial  $C$  typically converges to the correct value in a few iterations.

The entire algorithm contains several parameters that require tuning.

In the first phase we must decide whether to compare neighboring images or the ones that are more distant in time. The size of blurring appears to be a less critical parameter; in all experiments (2 different type of microscopes, 4 different types of cells) the same value provided in Sec. 2.1 was utilized. The thresholding step in the first phase is without any parameters.

Blurring in the second phase depends on the size (microscope magnification) and type of the cells. The proposed algorithm is not excessively sensitive to blurring size variations.

Most of the parameters are present in the third correction phase. The impact of the third phase depends on the quality of the original. When the motion of the cells is moderate and no debris and/or out-of-focus objects are present in the data virtually no correction is required in this phase. On the other hand, when the data contain a significant amount of irregularities, proper setting of correction parameters can improve the segmentation.

Experimental evaluation indicates that the algorithm is fairly robust with respect to the choice of parameters and that only one set of parameters is necessary for all images captured under similar conditions (the same type of microscope, the same frame rate and a similar type of cells).

Unlike other methods, our algorithm is capable of detecting only living cells and ignores the dead cells. This feature is used in cytotoxicity assessment as will be explained in Sec. 3.4.

## 3 Results

We tested our method’s ability to judge the biocompatibility status of materials. We conducted several experiments (and divided this section accordingly): First we compared the segmentation results of our algorithm with the manually segmented images and rated the similarity numerically (Section 3.1). In the second experiment (Section 3.2), we measured the performance of the segmentation methods using a qualitative research methodology. The third part (Section 3.3) focuses on processing of complete series of images and shows the connection to the biocompatibility assessment task. The last part shows the benefits of time-lapse imaging compared to conventional methods.

Before we present the results of the experiments we specify our experimental setting. We tested our algorithm on two different phase contrast microscopes and several types of

cancer cells. For evaluation of the quality of our algorithm (sections 3.1 and 3.2) we have chosen 70 images captured by two different microscopes: Nikon Biostation and Olympus X51S8F-3. We tested images of four cell types: MG63 human osteosarcoma, G10 human gingiva, HeLa cervix epitheloid carcino and L929 mouse fibroblasts. The magnification of the microscopes was  $20\times$ , each experiment lasted from 3 to 5 days, time interval between the images was 2 minutes, the resolution of the images was  $1280 \times 960$  (Biostation) and  $2288 \times 1712$  (Olympus). The cell lines were maintained at  $37^\circ$  C, 5%  $\text{CO}_2$  level and 95% humidity using an incubation chamber. For our evaluation we chose images evenly spaced throughout the entire time sequence to include the majority of potential cases: initial states where cells are undilated and circular, usual variants where most of the cells are separated, situations where the cells are arranged in large clusters covering most of the field of view. All the data used for the development and testing of the method were collected during the cytotoxicity test performed by the Working place of tissue culture certified laboratory.

Manual processing of images is a very tedious and time-consuming process. Results depend on the thoroughness of the human operator and could be biased due to subjective preferences and perception.

Each image was manually segmented by two experts and to annotate all the tested images it took about 12 hours. Interestingly the similarity of the manual segmentation was 94.8% (94.8% of pixels were labeled to the same category). More detailed information on the precision of manual labeling together with the evaluation of the algorithm precision is presented in Tab. 1. The segmentation sometimes also differs in discrimination between live and dead cells. In the case of L929 cells where the accuracy decreases below 90 percent the largest mistake results from tracing tentacles of the cells (see Fig. 1).

The proposed automatic segmentation algorithm was implemented in Matlab using various built-in functions. The CPU time (using Dual core 2.30 GHz) for segmentation of a single frame was 1.0 s for  $1280 \times 960$  and 4.0 s for  $2288 \times 1712$ .

For comparison, we tested three different methods. The first one [Seroussi et al., 2012] is based on active contours. Though this method segmented accurately some cells or cell clusters, many other cells were completely ignored, which resulted in a poor overall score. Therefore, we did not include results of this method in Tab. 1. Manual initialization of active contours can improve precision, however, this is a very time consuming step and comparable to fully manual segmentation, which renders active contours impractical for this task.

The other two methods are based on image filtering and consecutive thresholding. The first one uses a local entropy filter and Otsu thresholding. It is implemented in a software TimeLapseAnalyzer [Huth et al., 2011] as a “woundhealing” algorithm (hereafter denoted as TLA). This method is primarily intended for a wound healing setting, however, it can be also applied to regular time-lapse experiments.

The last method [Juneau et al., 2013] uses a range filter (finds maximum and minimum value in the neighborhood; this method is hereafter denoted as MinMax) and threshold-

ing is performed by a fixed threshold. Parameters of the TLA method are defined in the software. Parameters of the MinMax method were set to maximize the accuracy of thresholding on testing data.

To compare these methods, we conducted several tests. The results were evaluated by human experts (see Sect. 3.2) and their accuracy was evaluated numerically (Sect. 3.1).

### 3.1 Numerical evaluation

To compare the manual labeling with the automated one, we use precision (P), recall (R) and F1 statistics defined as:  $P = |TP|/(|TP| + |FP|)$ ,  $R = |TP|/(|TP| + |FN|)$ , F1-measure is the harmonic mean of precision and recall. Abbreviations TP, FN and FP denote true positive, false negative and false positive number of pixels classified in this way, respectively. In addition, we calculated the coverage curves on the labeled data and used correlation to measure the similarity of the curves.

First we compared two manually labeled sets. We considered the first one as the ground truth and the second one as tested segmentation. If we swapped the roles, the precision and recall values would be swapped too, but the F1 statistic remains the same.

We compared segmentation results of the tested algorithms with both manual ones. For comparison of manual vs. automated labeling, we calculated the statistics twice, once for each manually labeled set. Then we considered only those with better correspondence (higher score) for each image. (We assumed that lower score was caused by random errors in manual labeling).

The results for each series are shown in Tab. 1.

Our method consistently scored better than the method from TLA. The largest difference occurred for images with very high coverage ( $> 95\%$ ), see Fig. 3. Our algorithm also handled better dead cells present in the images. The MinMax method performed better than the TLA method but slightly worse than our method (despite the fact that we optimized all parameters of the MinMax method).

In the case of the HeLa cells our method was approximately as accurate as manual labeling. The coverage curves computed by our algorithm fit the ground truth ones very tightly. This qualifies our method as a good candidate to substitute manual labeling in determining the growth rate.

The numerical values from our evaluation cannot be compared with results in the literature. The accuracy depends highly on the type of the cells and of the microscope and, therefore, comparison with previously published results is very problematic.

### 3.2 Evaluation by Human Experts

Numerical evaluation using  $P, R$  and  $F1$  describes only some aspects of the segmentation accuracy. There are many other criteria such as number of components, length and smoothness of borders, etc., which are important but are ignored by these objective ratios.

**Table 1.** Numerical evaluation of the manual labeling, our algorithm, the TLA algorithm and the MinMax algorithm. P, R, F1 and cor stands for Precision, Recall, F1 measure and correlation of coverage curves.

Data	Statistic	MG63	G10	HeLa	L929
Manual labeling	P	0.90	0.96	0.95	0.88
	R	0.94	0.94	0.97	0.91
	F1	0.92	0.95	0.96	0.89
	cor	0.9962	0.9833	0.9996	0.9920
Our algorithm	P	0.88	0.91	0.97	0.61
	R	0.84	0.93	0.93	0.71
	F1	0.86	0.92	0.95	0.66
	cor	0.9847	0.9886	0.9995	0.8904
TimeLapseAnalyzer	P	0.64	0.79	0.90	0.54
	R	0.86	0.93	0.88	0.62
	F1	0.73	0.86	0.88	0.57
	cor	0.9694	0.9739	0.6615	0.5675
MinMax method	P	0.81	0.90	0.89	0.50
	R	0.76	0.91	0.93	0.88
	F1	0.77	0.91	0.91	0.63
	cor	0.8306	0.9456	0.9958	0.7719

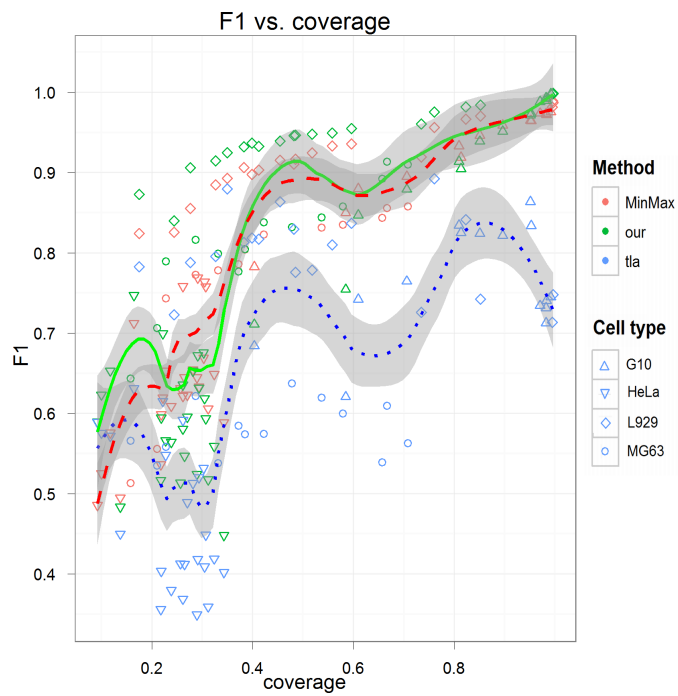


**Figure 3.** Dependence of the algorithm accuracy on the coverage. Colors correspond to the individual methods, mark shapes to the cell types. Local regression curves are dashed for MinMax method, solid for ours and dotted for TLA, dark strips correspond to 95 % confidence intervals of local regression curves.

**Table 2.** Human experts were asked to rank segmentation results (both manual and automated) for each tested image from best to worst.

Ranked:	best	2 <sup>nd</sup>	3 <sup>rd</sup>	worst
Manual labeling 1	40.4%	22.8%	27.2%	9.6%
Manual labeling 2	23.5%	33.8%	21.3%	21.3%
Our algorithm	24.3%	23.5%	30.9%	21.3%
TLA	11.8%	19.9%	20.6%	47.6%

Manual segmentation may vary from person to person, which is also the case here as was shown in the previous section. We were interested in the way how the experts evaluate themselves and we therefore asked them to rank the quality of the segmentation.

For each test image, we obtained four different segmentation outputs (two from human experts, one from our algorithm and one from the TLA algorithm; we omitted MinMax method here). We asked the human experts (the same who performed the original manual segmentation) to rank the segmentation results from best to worst. The experts did not have any information on the origin of the segmentation. The segmentation results were displayed to the experts in random order and were different for each image. The final ranking of both evaluators was very similar and Tab. 2 shows the average ranking of both evaluators.

The TLA algorithm scored the worst. In almost half the cases its segmentation was marked as the worst and the number of the segmentation results rated the best is very low (about 12 percent).

Manual segmentation ranked on the top, but interestingly both experts preferred labeling performed by the first expert.

An important observation is that our algorithm was evaluated comparably well as the manual labeling 2. Our algorithm is the first or second best ranked in almost 50% of the cases, which means that in half of the cases our segmentation was better than any of the two manual ones.

### 3.3 Single Cell Case

The analysis of another image series (HeLa cell line, 4 days long experiment, 37° C, 5% CO<sub>2</sub> level, 95% humidity, Olympus microscope, 20×) capturing life of a single cell and its descendants yielded another interesting result. We took a sequence of 3000 images that starts with a single cell and cover 12 mitotic divisions, and applied our segmentation algorithm to track cell coverage. Figure 5 shows the coverage in time as well as the time interval of mitotic events. We can see that our segmentation algorithm is sensitive to the area reduction of the cell during its mitotic phase. (Mitotic interval are highlighted by

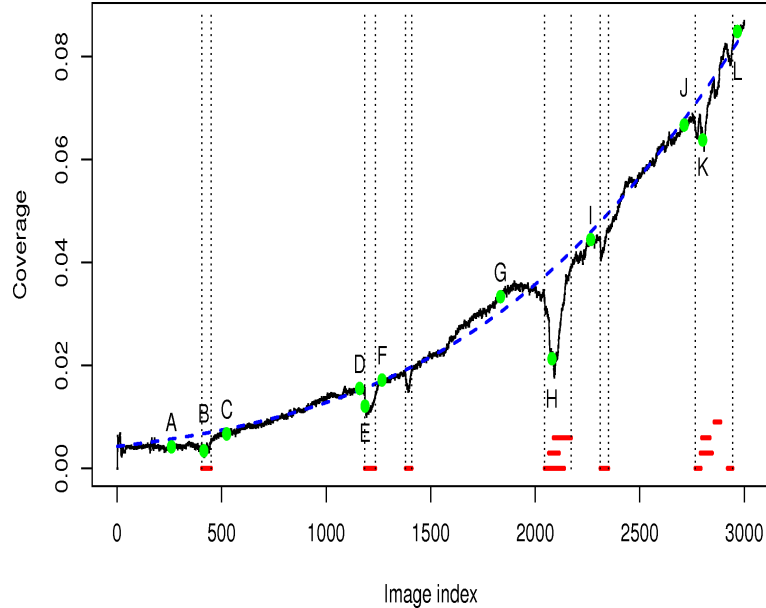


**Figure 4.** Human experts were asked to rank segmentation results (both manual and automated) for each tested image from best to worst.

horizontal bars under the curve and dashed vertical lines. There are exactly 12 bars that correspond to 12 mitotic divisions.) The detail of images labeled by dots and letters in Fig. 5 are presented in Fig. 6. We observe that depressions in the coverage curve in Fig. 5 truly correspond to actual changes in cell sizes.

This series of images is an ideal material to study the dynamics of the cell growth. There is only one group of cells, that do not touch the edges of the image, no other cells migrate to the field of view and the series is long enough to obtain sufficient data for statistical analysis.

Verhulst's logistic model of population growth [Verhulst, 1838] is one of frequently used population models. It can be presented in the form of a differential equation

$$\frac{dC(t)}{dt} = rC(t) \left( 1 - \frac{C(t)}{K} \right) , \quad (1)$$

where  $C$  is the population (coverage in our case) in time  $t$ ,  $r$  intrinsic growth rate and  $K$  is the carrying capacity of the environment. This differential equation has an analytical solution

$$C(t) = \frac{K}{1 + AKe^{-rt}} , \quad (2)$$

where  $A = 1/C(0) - 1/K$  is determined by the initial condition  $C(0)$ .

We tried to fit the coverage curve by Eqn. (2) (blue dashed line in Fig. 5). We can

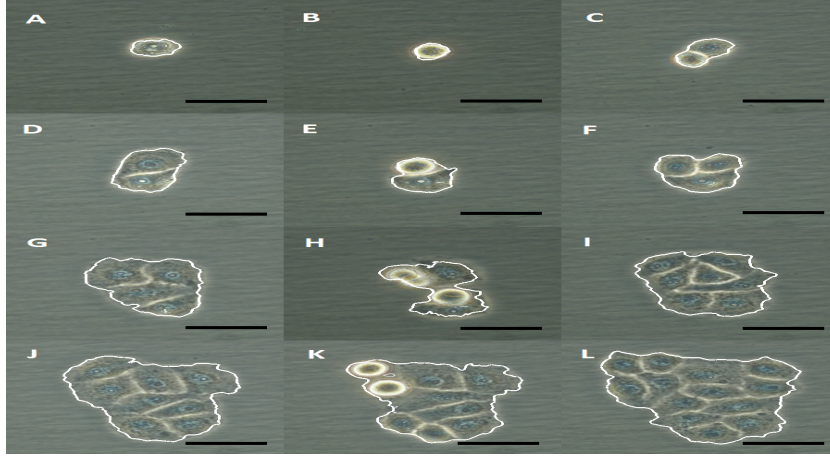


**Figure 5.** Time coverage curve (black) with labeled mitosis intervals (red) and logistic fit (blue dashed line). States in the marked moments (green dots) are shown in Fig. 6.

see that the fit is very accurate. Despite the fact the Verhulst model is usually used for a large number of individuals it can be used in this case to characterize the growth of a few cells.

This experiment demonstrates that the Verhulst model can be used to fit the coverage curves estimated with our segmentation algorithm. The Verhulst model fits well with the measured data (curve coverage). In this model the rate of growth is described by a single parameter  $r$ . Thus, using our algorithm, we can describe the dynamics of the cell growth using a single parameter. In addition, this parameter can be determined fully automatically without any intervention by a human operator.

This data series represents, in our opinion, an ideal benchmark test for cell segmentation algorithms. Therefore, we placed the original data together with our algorithm on our website <http://www.frov.jcu.cz/software/SegmentationTool>.

### 3.4 Estimation of $LT_{50}$

The standard approach to cytotoxicity assessment is to analyze results of an experiment at a single time instance (usually 24 hours after the start of the experiment). [ISO 10993-5, 2009] Time-lapse imaging could surpass the standard approach in two ways:

1) It can provide preliminary results in less time. When the tested material is toxic, the growth curve at a certain moment stops to follow the logistic curve (usually earlier than after 24 hours).

2) When the tested sample is extremely toxic, after 24 hours there will be no living cells. In this case the time-lapse imaging is more sensitive. This feature is illustrated in the following experiment.

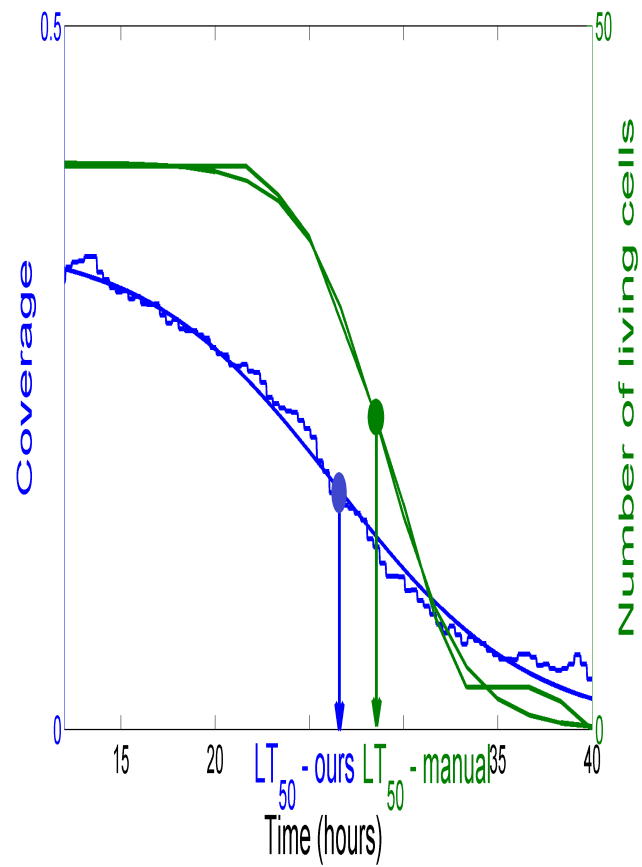


**Figure 6.** Region of interest for frames labeled in Fig. 5. State before (left column), during (central column) and after (right column) the mitosis event.

**Table 3.** Estimation of  $LT_{50}$  obtained by fitting the coverage curves and the ground truth  $LT_{50}$  obtained by manual cell counting.

Tested sample Cell line	Acorus celamus HeLa				CuSO <sub>4</sub> MG63		Gingko biloba L929		
$LT_{50}$ our (h)	54.5	60.2	47.4	61.2	26.8	28.7	8.4	13.7	11.3
$LT_{50}$ manual (h)	50.7	57.6	47.7	57.8	28.9	27.8	5.3	17.7	14.9

In total, 9 image series were acquired by testing three substances (extracts of Acorus celamus, Gingko biloba and solution of CuSO<sub>4</sub> at different concentrations) using three different cell lines - HeLa, MG63 and L929. The experiments lasted from 3 to 5 days (37° C, 5% CO<sub>2</sub> level, 95% humidity), the images were taken by Biostation microscope, using 20× objective.

We segmented the image by our method and the resulting coverage curves were fitted with the logistic curve. The key parameter was the time when the logistic curve reached its inflection point. This time instance we took as the estimation of  $LT_{50}$  (median lethal time). The ground truth was obtained by manually counting the number of cells in every image of the series. Our approach is illustrated in Fig. ??, the results are in Tab. 3.

$LT_{50}$  values automatically estimated by using our method are very close to the ground truth values. The absolute error (differences in  $LT_{50}$  estimated by the manual and automatic counting) is relatively low,  $\pm 4$  hours. However, the last three values (Gingko biloba) show a larger relative error (the ratio of estimated  $LP_{50}$ ), which is probably due to the fact that the extinction rate of cells was very high and it was difficult to visually determine their status (whether the cell is live or dead).

## 4 Conclusion

We developed a novel algorithm for segmentation of cells from time-lapse images acquired by phase contrast microscopes. The algorithm is based on processing of time differences between images and on a combination of thresholding, blurring and morphological operations. Presented results demonstrate that the proposed algorithm can be applied to a wide range of cell types. Due to its low time complexity it may be also suitable as a preprocessing (initialization) step for certain level-set methods.

We performed an analysis of manual labeling focused on its precision. We compared the precision of our algorithm with the manual one and concluded that the performance of our algorithm is similar to the performance of a human operator. The evaluation suggests that our algorithm can be a good substitute for manual labeling.

We showed that the time-lapse imaging may help in the assessment of cytotoxicity

using the coverage curve fitting with the Verhulst's logistic model. Our method detects only living cells. In combination with another segmentation method, it could serve as a detector of the ratio between live and dead cells. We plan to test this possibility in the future.

We have implemented the method in a stand-alone program that is free to download on the homepage of our project <http://www.frov.jcu.cz/software/SegmentationTool>. The program is currently being tested by the Working place of tissue culture - certified laboratory of the Institute of Complex Systems, University of South Bohemia, Czech Republic.

## 5 Acknowledgement

The study was financially supported by the Ministry of Education, Youth and Sports of the Czech Republic - projects 'CENAKVA' (No. CZ.1.05/2.1.00/01.0024), 'CENAKVA II' (No. LO1205 under the NPU I program), the GAUK grant No. 914813/2013, the grant GAČR No. 13-29225S and the grant SVV2015260223. The authors would also like to thank the staff of the Working place of tissue culture - certified laboratory at Nové Hradky, namely Monika Homolková and Šárka Beranová for their assistance with the manual segmentation of the cells.

## References

- M E Ambühl, C Brepsant, J-J Meister, a B Verkhovsky, and I F Sbalzarini. High-resolution cell outline segmentation and tracking from phase-contrast microscopy images. *Journal of microscopy*, 245(2):161–70, March 2012. ISSN 1365-2818. doi: 10.1111/j.1365-2818.2011.03558.x. URL <http://www.ncbi.nlm.nih.gov/pubmed/21999192>.
- C J Bradhurst, W Boles, and Yin Xiao Yin Xiao. Segmentation of bone marrow stromal cells in phase contrast microscopy images, 2008. URL <http://ieeexplore.ieee.org/lpdocs/epic03/wrapper.htm?arnumber=4762144>.
- M Červinka and V Púža. In vitro toxicity testing of implantation materials used in medicine: Effects on cell morphology, cell proliferation and dna synthesis. *Toxicology in Vitro*, 4(4):711–716, 1990.
- Chung-Ho Chen and Sumi C. Chen. Cell growth factor activity: New quantitative method in cell culture assay. *Experimental Cell Research*, 136(1):43 – 51, 1981. ISSN 0014-4827. doi: [http://dx.doi.org/10.1016/0014-4827\(81\)90036-7](http://dx.doi.org/10.1016/0014-4827(81)90036-7). URL <http://www.sciencedirect.com/science/article/pii/0014482781900367>.
- I Ersoy, F Bunyak, M A Mackey, and K Palaniappan. Cell segmentation using hessian-based detection and contour evolution with directional derivatives. In *Image Processing, 2008. ICIP 2008. 15th IEEE International Conference on*, volume 2008, pages 1804–1807. IEEE, 2008. ISBN 9781424417650. doi: 10.1109/ICIP.2008.4712127. URL [http://ieeexplore.ieee.org/xpls/abs/\\_all.jsp?arnumber=4712127](http://ieeexplore.ieee.org/xpls/abs/_all.jsp?arnumber=4712127).
- Johannes Huth, Malte Buchholz, Johann M Kraus, Martin Schmucker, Götz Von Wichert, Denis Krndija, Thomas Seufferlein, Thomas M Gress, and Hans A Kestler. Significantly improved precision of cell migration analysis in time-lapse video microscopy through use of a fully automated tracking system. *BMC Cell Biology*, 11(1): 24, 2010. URL <http://www.pubmedcentral.nih.gov/articlerender.fcgi?artid=2858025&tool=pmcentrez&rendertype=abstract>.
- Johannes Huth, Malte Buchholz, Johann M Kraus, Kristian Mø lhave, Cristian Gradi-naru, Götz v Wichert, Thomas M Gress, Heiko Neumann, and Hans a Kestler. Time-lapseanalyzer: multi-target analysis for live-cell imaging and time-lapse microscopy. *Computer methods and programs in biomedicine*, 104(2):227–34, November 2011. ISSN 1872-7565. doi: 10.1016/j.cmpb.2011.06.002. URL <http://www.ncbi.nlm.nih.gov/pubmed/21705106>.
- ISO 10993-5. Biological evaluation of medical devices. tests for in vitro cytotoxicity., 2009.

- Pierre-Marc Juneau, Alain Garnier, and Carl Duchesne. Selection and tuning of a fast and simple phase-contrast microscopy image segmentation algorithm for measuring myoblast growth kinetics in an automated manner. *Microscopy and Microanalysis*, 19:855–866, 8 2013. ISSN 1435-8115. doi: 10.1017/S143192761300161X. URL [http://journals.cambridge.org/article\\_S143192761300161X](http://journals.cambridge.org/article_S143192761300161X).
- Takeo Kanade, Zhaozheng Yin, Ryoma Bise, Seungil Huh, Sungeun Eom, Michael F. Sandbothe, and Mei Chen. Cell image analysis: Algorithms, system and applications. *2011 IEEE Workshop on Applications of Computer Vision (WACV)*, pages 374–381, January 2011. doi: 10.1109/WACV.2011.5711528. URL <http://ieeexplore.ieee.org/lpdocs/epic03/wrapper.htm?arnumber=5711528>.
- Fuhai Li, Xiaobo Zhou, Hong Zhao, and Stephen T C Wong. Cell segmentation using front vector flow guided active contours. *Medical Image Computing and Computer-Assisted Intervention*, 12(Pt 2):609–616, 2009. URL <http://www.pubmedcentral.nih.gov/articlerender.fcgi?artid=2896022&tool=pmcentrez&rendertype=abstract>.
- Kang Li, Eric D Miller, Lee E Weiss, Phil G Campbell, and Takeo Kanade. Online tracking of migrating and proliferating cells imaged with phase-contrast microscopy. In *Computer Vision and Pattern Recognition Workshop, 2006. CVPRW'06. Conference on*, pages 65–65. IEEE, 2006.
- John R Masters. Hela cells 50 years on: the good, the bad and the ugly. *Nature Reviews Cancer*, 2(4):315–319, 2002.
- N Otsu. A threshold selection method from gray-level histograms. *Automatica*, 20(1):62–66, 1975. URL <http://www.tecgraf.puc-rio.br/~mgattass/cg/trbImg/Otsu.pdf>.
- Jiyan Pan, Takeo Kanade, and Mei Chen. Learning to detect different types of cells under phase contrast microscopy. *Microscopic Image Analysis with Applications in Biology*, pages 1–8, 2009.
- Jiyan Pan, Takeo Kanade, and Mei Chen. Heterogeneous conditional random field: Realizing joint detection and segmentation of cell regions in microscopic images. In *Computer Vision and Pattern Recognition (CVPR), 2010 IEEE Conference on*, pages 2940–2947. IEEE, June 2010. ISBN 978-1-4244-6984-0. doi: 10.1109/CVPR.2010.5540037. URL <http://ieeexplore.ieee.org/lpdocs/epic03/wrapper.htm?arnumber=5540037>.
- Huiming Peng, Xiaobo Zhou, Fuhai Li, Xiaofeng Xia, and S T C Wong. Integrating multi-scale blob/curvilinear detector techniques and multi-level sets for automated segmentation of stem cell images. In *Biomedical Imaging: From Nano to Macro, 2009. ISBI'09. IEEE International Symposium on*, pages 1362–1365, 2009. ISBN 9781424439317. doi: 10.1109/ISBI.2009.5193318.

- I Seroussi, D Veikherman, N Ofer, S Yehudai-Resheff, and K Keren. Segmentation and tracking of live cells in phase-contrast images using directional gradient vector flow for snakes. *Journal of microscopy*, 247(2):137–46, August 2012. ISSN 1365-2818. doi: 10.1111/j.1365-2818.2012.03624.x. URL <http://www.ncbi.nlm.nih.gov/pubmed/22591174>.
- J Soukup, P Cisar, and F Sroubek. Segmentation of time-lapse images with focus on microscopy images of cells. In Alfredo Petrosino, editor, *17th International Conference on Image Analysis and Processing - ICIAP 2013*, volume 8157, Part II of *LNCS*, pages 71–80, Berlin, Heidelberg, 2013. Springer-Verlag.
- P F Verhulst. Notice sur la loi que la population suit dans son accroissement. *Corr Math et Phys*, 10(10):113–121, 1838. URL <http://scholar.google.com/scholar?hl=en&btnG=Search&q=intitle:Notice+sur+la+loi+que+la+population+suit+dans+son+accroissement#0>.
- Zhaozheng Yin and Takeo Kanade. Restoring artifact-free microscopy image sequences. In *Biomedical Imaging: From Nano to Macro, 2011 IEEE International Symposium on*, pages 909–913. IEEE, 2011.
- Zhaozheng Yin, Ryoma Bise, Mei Chen, and Takeo Kanade. Cell segmentation in microscopy imagery using a bag of local bayesian classifiers. In *Biomedical Imaging: From Nano to Macro, 2010 IEEE International Symposium on*, pages 125–128. IEEE, 2010. ISBN 9781424441266.
- Zhaozheng Yin, Takeo Kanade, and Mei Chen. Understanding the phase contrast optics to restore artifact-free microscopy images for segmentation. *Medical image analysis*, 16(5):1047–62, July 2012. ISSN 1361-8423. doi: 10.1016/j.media.2011.12.006. URL <http://www.ncbi.nlm.nih.gov/pubmed/22386070>.
- Christophe Zimmer, Elisabeth Labruyère, Vannary Meas-Yedid, Nancy Guillén, and Jean-Christophe Olivo-Marin. Segmentation and tracking of migrating cells in videomicroscopy with parametric active contours: a tool for cell-based drug testing. *IEEE transactions on medical imaging*, 21(10):1212–21, October 2002. ISSN 0278-0062. doi: 10.1109/TMI.2002.806292. URL <http://www.ncbi.nlm.nih.gov/pubmed/12585703>.